

The Highly Efficient Inorganic SrF₂:Gd³⁺, Eu³⁺ Phosphor for Mercury-Free Fluorescence Lamps

S.R. Jaiswal^{1,a*}, N.S. Sawala^{2,b}, P.A. Nagpure^{3,c}, W.S. Barde^{4,d},
S.K. Omanwar^{5,e}

¹Department of Physics, Shri R.L.T. College of Science, Akola. 444001(INDIA)

²Department of Science and Humanities Government Polytechnic, Arvi, Wardha 442201 (INDIA),

³Department of Physics, Shri Shivaji Science College, Amravati. 444602 (INDIA)

⁴Department of Physics, Shri Shivaji Science College, Amravati. 444602 (INDIA)

⁵Department of Physics, Sant Gadge Baba Amravati University, Amravati. 444602 (INDIA)

^{a*}srjaiswal07@gmail.com, ^bprincipal.gparvi@temaharashtra.gov.in,

^cshivajiscamt.office@gmail.com, ^dwamanbarde81@gmail.com, ^ehodphysic@sgbau.ac.in

Keywords: Visible Quantum Cutting, Down-conversion, Vacuum Ultraviolet (VUV) spectroscopy, Mercury Free fluorescent lighting (MFFL), Quantum Efficiency.

Abstract. The strong vacuum ultraviolet (VUV) radiation absorption and energy transfer mechanism are detected in SrF₂: Gd³⁺, Eu³⁺ fluoride phosphor. The phosphor is synthesized by a wet chemical method followed by a reactive atmospheric process (RAP). The Powder XRD analysis shows structural purity. The photoluminescence characteristics of SrF₂:Gd³⁺, Eu³⁺ phosphor is studied using the remote access of 4B8 window (VUV beamline) of the Beijing Synchrotron Radiation Facility (BSRF) China. In this paper, the energy transfer mechanism from the Gd³⁺ to Eu³⁺ through the cross-relaxation process is investigated. The down-conversion of energy from VUV (142 nm) to visible with a quantum efficiency (QE) of around 124% has been detected. The PL excitation and emission characteristics of the prepared phosphor advocate it as a prominent material for applications in mercury-free fluorescent lighting (MFFL) & Plasma Display panels.

Introduction

In recent times, for the development of MFFL and plasma display panel (PDP) technology, new quantum cutting (two-photon luminescent) phosphors are becoming essential for the realization of highly resourceful luminescent materials under VUV excitation. The emission of two or more low energy photons for each high energy absorbed photon is termed quantum cutting mechanism. It is also known as a down-conversion (DC) mechanism with quantum efficiency greater than 100% and it deals with the vision of providing improved energy efficiency in lighting devices [1]. The VUV levels of many of the lanthanide ions have been recently measured, thereby providing the starting point from which new phosphors may be designed [2]. Shi. et al. reported that the visible quantum cutting via downconversion has been observed in BaF₂: Gd, Eu phosphor. The inorganic barium fluoride (BaF₂) host matrix has a wide energy band gap, having an energy gap of about 10.9 eV [3]. So that BaF₂:RE³⁺ (Ce, Pr, Tb, Eu, Dy) have been premeditated in some earlier reports [4-6]. On the same ground, in the present experiment Gadolinium (Gd) and Europium (Eu) are used as dopants in the SrF₂ host and excitation at the VUV range is anticipated.

The process of quantum cutting through downconversion in SrF₂ can occur by the combination of Gd³⁺ and Eu³⁺, in which Gd³⁺ acts as a sensitizer and Eu³⁺ acts as an activator. The current report presents the results of down-conversion luminescence for SrF₂: Gd³⁺, Eu³⁺ synthesised by the soft chemical route and the subsequent heating in the reactive atmosphere. The resulting fine powder was tested for the purity of phase by the XRD technique. The VUV excitation and emission properties are investigated through remote access of the 4B8 VUV spectroscopy beamline of BSRF, Institute of High Energy Physics in Beijing, China.

Materials and Methods

The overall synthesis process is illustrated in the following flow chart (fig.1). Strontium fluoride co-doped with Gd^{3+} , Eu^{3+} phosphor synthesis by the wet chemical path and subsequently heated into a reactive atmosphere. In the synthesis process, analytical grade strontium carbonate ($SrCO_3$) is used as a precursor. The hydrofluoric acid (HF) was added slowly to a homogeneous mixture of strontium carbonate and double-distilled (DD) water in a Teflon beaker. The slurry so formed was dried by warming it on a hot plate at $80^\circ C$. The aqueous solution of nitrate salts of gadolinium and europium obtained by boiling gadolinium and europium oxides (AR grade) separately in nitric acid was added in specified amounts to a mixture in a Teflon beaker. The mixture is then dried to get a fine powder.

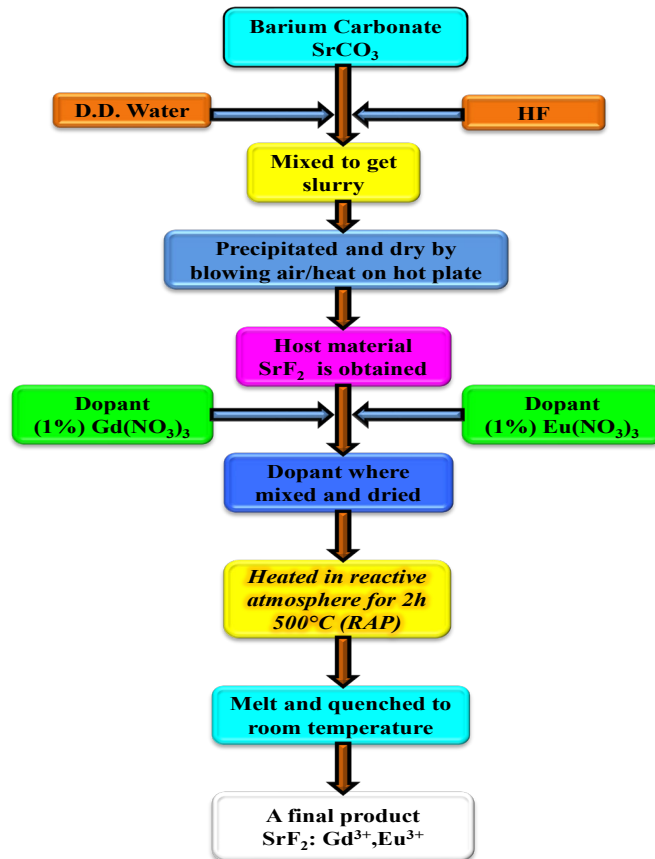


Fig.1 Flow chart of synthesis of SrF₂: Gd³⁺, Eu³⁺ phosphor.

The powder was then heated in a sealed glass tube under the reactive atmosphere created by a suitable amount of ammonium fluoride. It was further heated in a graphite crucible for 1 hour at a suitable temperature [7].

Results and Discussion

XRD Analysis:

The synthesised fine powder of doped and undoped SrF₂ are tested for the purity of phase by x-ray diffraction (XRD) technique as shown in Fig.2.

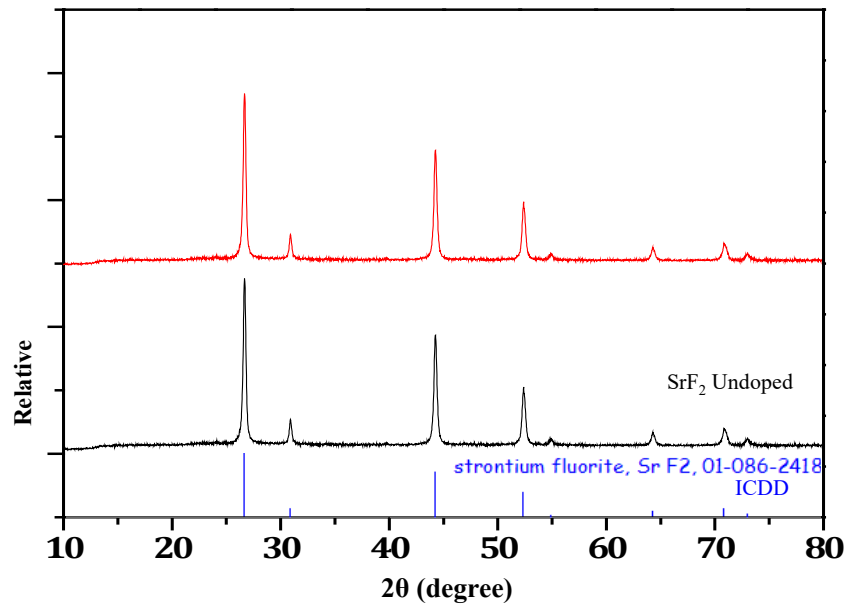


Fig.2 XRD patterns of doped and undoped SrF₂

The XRD pattern for doped and undoped SrF₂ is found to be the same and agrees well with the standard data from the ICDD file (01-086-2418). Also the XRD pattern shows that SrF₂ lattice possesses cubic structure with a space group Fm-3m (225) with unit cell parameter $a = b = c = 5.7912 \text{ \AA}$ and $\alpha = \beta = \gamma = 90^\circ$. The diffraction peaks in all the cases are indexed to a pure cubic structure of SrF₂ without the existence of any auxiliary phases. The average crystallite size calculated from the Scherrer formula is 23 nm and the strain calculated corresponding to the shift in (111) peak of XRD is 0.0007 [8].

VUV Photoluminescence Studies & Quantum Cutting:

It can be observed from Fig.3 that at 1 mol% of Gd³⁺ ions in the SrF₂ host matrix shows an optimum intensity peak at 311 nm at the excitation of 273 nm. Thus Gd³⁺ shows concentration quenching as a sensitizer in the SrF₂ host matrix for higher concentrations. Fig. 4 shows excitation lines peaking at about 142, 156, 204 and 274 nm responsible for ⁸S_{7/2}→⁶G_J, ⁶D_J, ⁶I_J transitions respectively. Fig. 5 shows emission bands underneath excitation of the wavelength 273, 156 and 142 nm. The prominent emission lines of Eu³⁺ peaked at 593, 613, 650 and 700 nm correspond to ⁵D₀→⁷F_J (J=0,1, 2, 3) transitions respectively. The ⁵D₀→⁷F_J transition peaks of Eu³⁺ are comparatively much more intense than that ⁵D₁→⁷F_J (J=0,1, 2, 3) of transitions as shown in Fig 5.

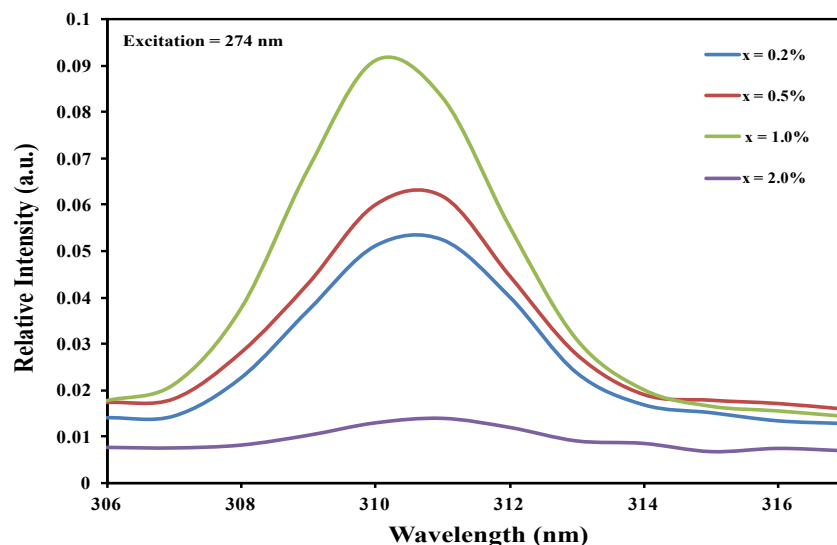


Fig.3 Emission spectra of SrF₂: x% Gd³⁺ under the excitation of 273 nm.

It can be seen that the natures of emission spectrums are identical. The emission intensities corresponding to all transitions of Eu^{3+} at 142 nm excitation are maximum.

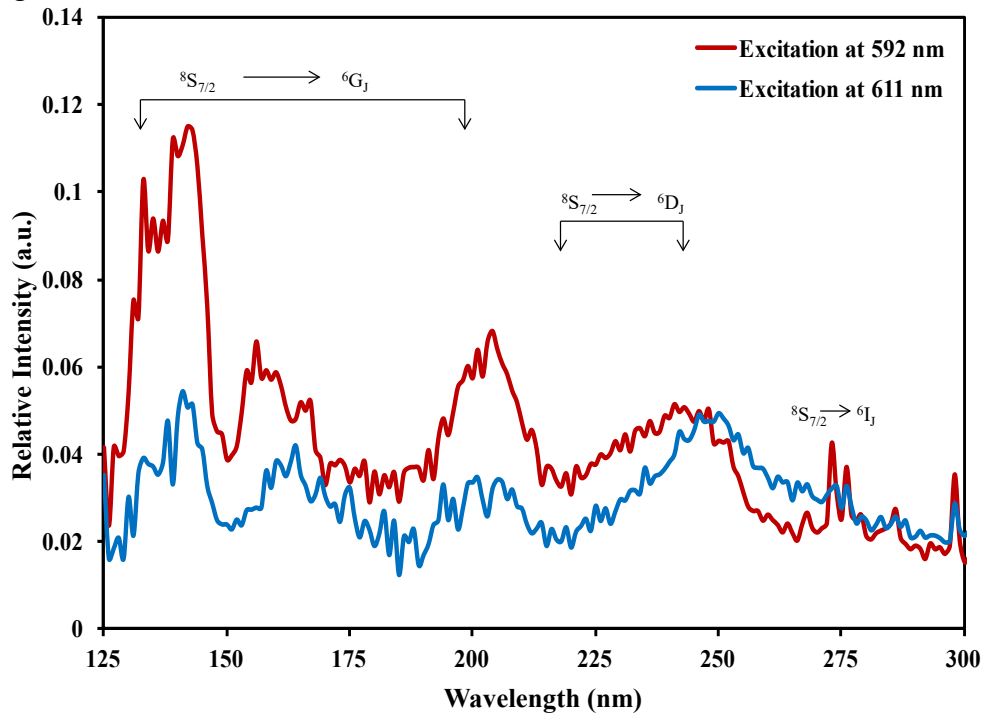


Fig.4 Excitation spectrum of $\text{SrF}_2: \text{Gd}^{3+}, \text{Eu}^{3+}$ observed at 593 and 611 nm.

The emission spectrums of the phosphor $\text{SrF}_2: \text{Gd}^{3+}, \text{Eu}^{3+}$, corresponding to the transitions of Eu^{3+} at three different excitation wavelengths (142, 156 & 273 nm) are depicted in Fig. 5.

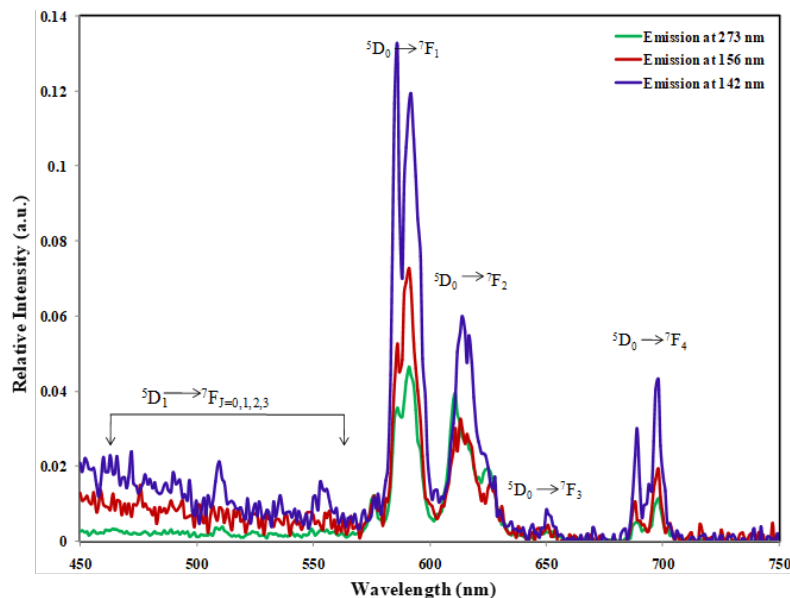


Fig.5 Emission spectra of $\text{SrF}_2: \text{Gd}^{3+}, \text{Eu}^{3+}$

The ratios of peak emission intensity values corresponding to ${}^5\text{D}_0 \rightarrow {}^7\text{F}_2$ (614 nm) and ${}^5\text{D}_0 \rightarrow {}^7\text{F}_1$ (592 nm) transitions are 0.50 and 0.85 respectively for 142 nm and 273 nm excitation wavelengths. This implies that magnetic dipole transitions ${}^5\text{D}_0 \rightarrow {}^7\text{F}_1$ become prominent compared to electric dipole transitions ${}^5\text{D}_0 \rightarrow {}^7\text{F}_2$ at VUV excitations (142 & 156 nm). The magnetic dipole transitions can occur only when Eu^{3+} locates at a site in the host with inversion symmetry [9]. Consequently, it may say that at VUV wavelengths the probability of transfer of excitation energy to the Eu^{3+} located at a site with inversion symmetry is more. The combination of Gd^{3+} and Eu^{3+} ions in the SrF_2 host matrix plays a very important role to form cross-relaxation energy transfer (CRET) and increasing the luminescence quantum efficiency beyond 100%.

The asymmetric ratio (luminescence intensity ratio R), which in the case of Eu^{3+} ions can be calculated from the expression $R = I(^5\text{D}_0 \rightarrow ^7\text{F}_2) / I(^5\text{D}_0 \rightarrow ^7\text{F}_1)$ [10]. From the integral intensities of the emission spectra, the asymmetric ratio is 0.5264 at 142 nm excitation wavelength. The process of absorption of VUV photon through $^8\text{S}_{7/2} \rightarrow ^6\text{G}_J$ transition of Gd^{3+} ions, transfer of energy to two Eu^{3+} ions leading $^7\text{F}_J \rightarrow ^5\text{D}_J$ transitions and emission of two visible red colour photons through $^5\text{D}_0 \rightarrow ^7\text{F}_J (J=0, 1, 2, 3)$ transition of Eu^{3+} ions as described in the energy level diagram [11].

As exemplified in Fig.6, CRET (step-1) can bring the Eu^{3+} ion only into $^5\text{D}_0$ excited state therefore emissions due to $^5\text{D}_0 \rightarrow ^7\text{F}_J (J=0, 1, 2, 3)$ transitions is only probable. As excited Eu^{3+} is responsible for the first visible photon, the first step is called flourishing energy migration. However in the direct energy transfer (step-2), all the excited states $^5\text{D}_J (J=0, 1, 2, 3)$ of Eu^{3+} are probable, so the emission lines corresponding to all $^5\text{D}_0 \rightarrow ^7\text{F}_J (J=0, 1, 2, 3)$ transitions are probable [11-14].

The PL emission spectra of SrF_2 doped with Gd^{3+} and Eu^{3+} (1 mol% each) in the entire visible range of wavelengths was monitored at 142, 156 and 273 nm excitations, to authenticate the energy transfer process and quantum cutting. The 142 nm excitations take Gd^{3+} to $^6\text{G}_J$ states while 273 nm excitations take to $^6\text{I}_J$ states. The two-step relaxation of Gd^{3+} and hence quantum cutting is impossible due to excitation at $^6\text{I}_J$ states. So the emissions corresponding to $^5\text{D}_0 \rightarrow ^7\text{F}_J (J=0, 1, 2, 3)$ transitions (step 2 in Fig. 6) of Eu^{3+} has a typical branching ratio between $^5\text{D}_0$ and other $^5\text{D}_J$ states. On the other hand, 142 nm excitation of Gd^{3+} to $^6\text{G}_J$ states ensures the quantum cutting via two-step energy transfer. It results in an increase in $^5\text{D}_0$ emissions over the typical branching ratio between $^5\text{D}_0$ and other $^5\text{D}_J$ states. This fact is used to calculate the luminescence quantum efficiency of the phosphor.

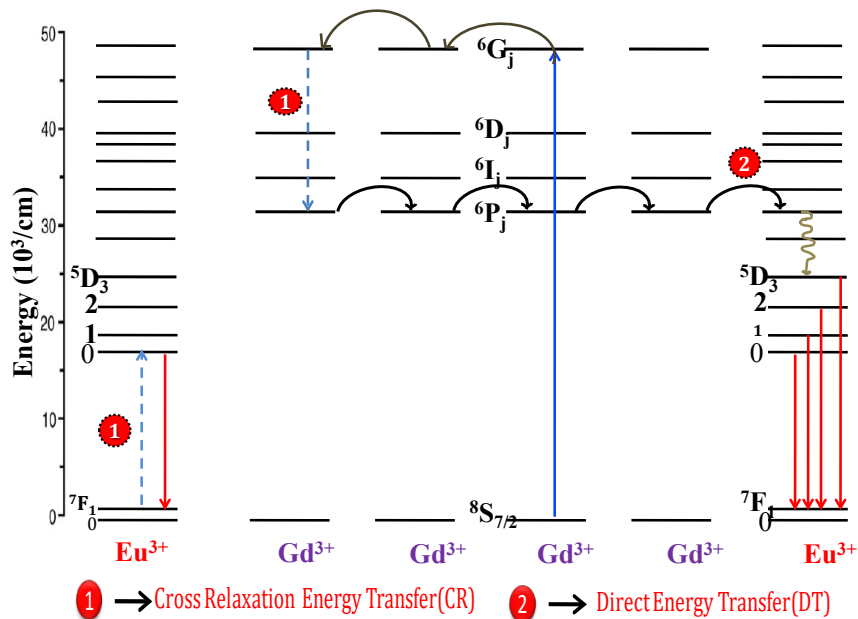


Fig.6 Energy level diagrams of Eu^{3+} and Gd^{3+} showing the cross-relaxation energy transfer process.

The colour quality of the as-synthesized phosphors will be primarily assessed by the CIE chromaticity coordinate (x , y). According to the emission spectrum of $\text{SrF}_2: \text{Gd}^{3+}, \text{Eu}^{3+}$, the chromaticity coordinates of this sample are found to be (0.46212 and 0.37291). The spectra $\text{SrF}_2: \text{Gd}^{3+}, \text{Eu}^{3+}$ fitted to CIE 1931 chromaticity diagram is shown in Fig 7 [15].

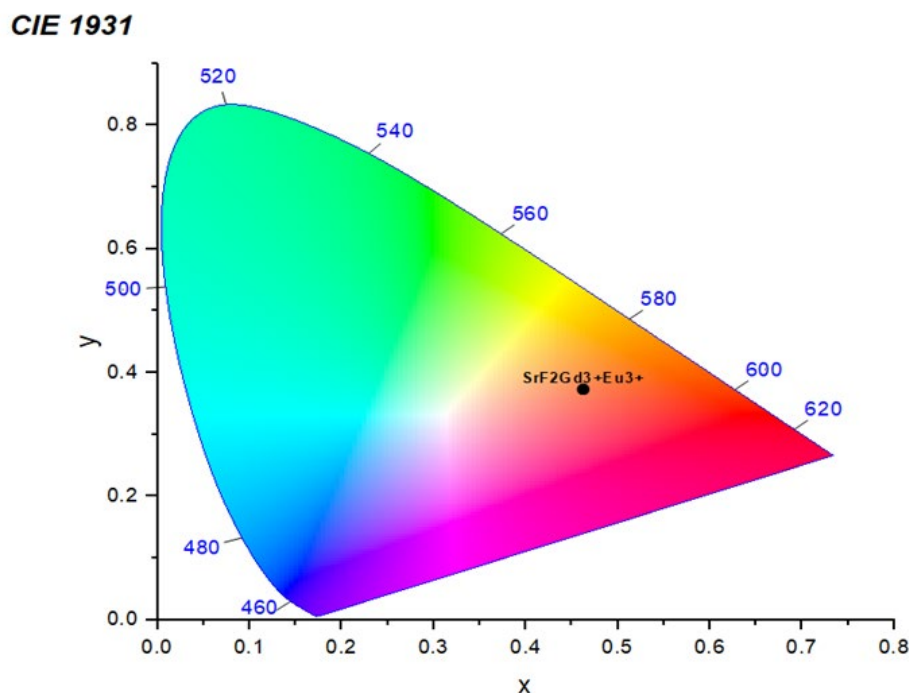


Fig. 7 The CIE chromaticity coordinates of red phosphor $\text{SrF}_2: \text{Gd}^{3+}, \text{Eu}^{3+}$

In this experiment, the quantum efficiency is calculated only for 142 nm excitation. To determine the efficiency of the cross-relaxation, the formula proposed by Wegh [16-19] is adopted as follows

$$\frac{P_1}{P_1 + P_2} = \frac{R_2 - R_1}{R_1 + 1}$$

Where, P_1 and P_2 are the probabilities of the energy transfer from Gd^{3+} to Eu^{3+} through cross-relaxation and the direct transfer respectively, $R_1 = ({}^5\text{D}_0/{}^5\text{D}_{1,2,3})/{}^6\text{I}_J$ and $R_2 = ({}^5\text{D}_0/{}^5\text{D}_{1,2,3})/{}^6\text{G}_J$ are the ratios of the ${}^5\text{D}_0$ and ${}^5\text{D}_{1,2,3}$ emission integral intensities. The subscript (${}^6\text{G}_J$ or ${}^6\text{I}_J$) represents the excitation level for which the ratio is detected. From the emission spectra, the values of R_1 and R_2 are found to be 0.2179 and 0.52064, respectively. Therefore, the value of $(P_1 / (P_1 + P_2))$ obtained is 0.24. This means that there are 24% (24/100) Gd^{3+} ions in the ${}^6\text{G}_J$ excited state that settle down through a two-step energy transfer by emitting two visible photons through Eu^{3+} transitions. So the overall quantum efficiency of the phosphor comes out to be 124%.

It should be noted that the incident VUV photon absorption efficiency has taken into consideration also some non-radiative losses at defects and impurities are disregarded, quantum cutting in the Gd to Eu understanding requires energy transfer over the Gd sublattice to Eu [13].

Conclusions

The inorganic material $\text{SrF}_2: \text{Gd}^{3+}, \text{Eu}^{3+}$ is successfully prepared by wet chemical method and subsequent heating in the reactive atmosphere. The XRD pattern confirms the cubic structure of SrF_2 . The visible quantum cutting and energy transfer through down-conversion are observed in $\text{SrF}_2: 1\% \text{Gd}^{3+}, 1\% \text{Eu}^{3+}$. The quantum efficiency is found to be around 124% under the VUV excitation of 142 nm. The PL characteristics and quantum efficiency of the synthesized phosphor at VUV wavelengths advocate its potential for applications in mercury-free fluorescent lighting.

Acknowledgements

The authors are thankful to the scientists at Beijing Synchrotron Radiation Facility (BSRF), the Republic of China for giving remote access to the facility for recording VUV emission and excitation spectra with beamline 4B8 under dedicated synchrotron mode.

References

- [1] C.R. Ronda, Phosphors for lamps and displays, *J. Alloys Compd.* 225 (1993) 534-538.
- [2] M. Y. William, *Phosphor Handbook*, CRC Press is an imprint of the Taylor & Francis Group, ISBN: 0-8493-3564-7.
- [3] B. Liu, Y. Chen, C. Shi, H. Tanga, Y. Tao, Visible quantum cutting in BaF₂: Gd, Eu via downconversion, *J. Lumin.*, 101 (2003) 155–159
- [4] B. Herden, A. García-Fuente, H. Ramanantoanina, T. Jüstel, C. Daul, W. Urland, Photon cascade emission in Pr³⁺ doped fluorides with CaF₂ structure: Application of a model for its prediction, *Chemical physics letter.* 620 (2015) 29-34.
- [5] W. Binder, S. Dislerhoff, J. Cameron, Dosimetric Properties of CaF₂: Dy, (a) Proc. II Int. Conf. on Lumin. Dosim. Gatlinberg, 1968, pp. 45–53; (b) *Health Phys.*, 1969, vol. 17, no. 4, pp. 613–618.
- [6] A.C. Lucas, R.H. Moss, B.M. Casper, Proc. Int. Conf. on Lumin. Dosim, Sao Paulo (Brazil), 1977, pp. 131- 139
- [7] P. Belsare, C. Joshi, S. Moharil, V. Kondawar, P. Muthal, S. Dhopte, Luminescence of Eu²⁺ in some fluorides prepared by reactive atmosphere processing, *J. Alloys Compd.* 450 (2008) 468–472.
- [8] A. King, R. Singh, R. Anand, S. K. Behera, B. B. Nayak, Spectroscopic studies of borohydride derived cerium doped zirconia nanoparticles under air and argon annealing conditions, *J.Nanopart Res* (2021) 23-156
- [9] J. Zhou, L. Xie, J. Zhong, H. Liang, J. Zhang, M. Wu, Site occupancy and luminescence properties of Eu³⁺ in double salt silicate Na₃LuSi₃O₉, *Optical Materials Express*, 8 (2018) 736-743.
- [10] K. Milewska, M. Maciejewski, A. Synak, M. Łapinski, A. Mielewczyk-Gryn, W. Sadowski, B. Koscielska, From Structure to Luminescent Properties of B₂O₃-Bi₂O₃-SrF₂Glass and Glass-Ceramics Doped with Eu³⁺ Ions, *Materials*, 14 (2021) 4490.
- [11] C. Feldmann, T. Jüstel, C.R. Ronda, D.U. Wiechert, Quantum efficiency of down-conversion phosphor LiGdF₄:Eu, *J. Lumin.*, 92 (2001) 245-254.
- [12] B. Liua, Y. Chena, C. Shia, H. Tanga, Y. Tao, Visible quantum cutting in BaF₂:Gd, Eu via downconversion, *J.Lumin.*, 101 (2003) 155–159.
- [13] R.T. Wegh, H. Donker, K. Oskam, and A. Meijerink, Visible quantum cutting in Eu³⁺-doped gadolinium fluorides via downconversion, *J. Lumin.*, 82 (1999) 93-104.
- [14] R. Singh, A. King, B. B. Nayak, Influence of calcination temperature on phase, powder morphology and photoluminescence characteristics of Eu-doped ZnO nanophosphors prepared using sodium borohydride, *J. Alloys Compd.*, 847(2020)156382.
- [15] R. Singh, A. King, B. B. Nayak, Phase evolution, powder morphology and photoluminescence exploration of borohydride derived red-emitting Eu³⁺ doped ZnO nanophosphors, *Materials Science in Semiconductor Processing* 133 (2021) 105969.
- [16] R.T. Wegh, H. Donker, K. Oskam, A. Meijerink, Visible quantum cutting in LiGdF₄:Eu³⁺ through downconversion, *Science* 283 (1999)663-666.

-
- [17] S.R. Jaiswal, N. S. Sawala, P.A. Nagpure, V. B. Bhatkar, S.K. Omanwar, Visible quantum cutting in Tb^{3+} doped $BaGdF_5$ phosphor for the plasma display panel, *J Mater Sci: Mater Electron* 28 (2017) 2407–2414
- [18] S.K. Omanwar, S.R. Jaiswal, N.S. Sawala, K.A. Koparkar, P.A. Nagpure, V. B. Bhatkar, Visible quantum cutting in green-emitting $BaF_2: Gd^{3+}, Tb^{3+}$ phosphor: An approach toward mercury-free lamps, *St. petrbergpolytechnical University Journal: Physics and Mathematics* 3 (2017) 218-224.
- [19] S.R. Jaiswal, N.S. Sawala, K.A. Koparkar, V. B. Bhatkar, S.K. Omanwar, Ultra-violet to visible quantum cutting in $YPO_4: Gd^{3+}, Tb^{3+}$ phosphor via down-conversion, *material discovery*, 7 (2017) 15-20.